


RESEARCH PAPER



## A study of Rose Bengal against a 2-keto-3-deoxy-D-manno-octulosonate cytidyltransferase as an antibiotic candidate

Suwon Kim, Seri Jo, Mi-Sun Kim and Dong Hae Shin 

Graduate School of Pharmaceutical Sciences, Ewha Woman's University, Seoul, Republic of Korea

### ABSTRACT

Frequent occurrences of multi-drug resistance of pathogenic Gram-negative bacteria threaten human beings. The CMP-2-keto-3-deoxy-D-manno-octulosonic acid biosynthesis pathway is one of the new targets for antibiotic design. 2-Keto-3-deoxy-D-manno-octulosonate cytidyltransferase (KdsB) is the key enzyme in this pathway. KdsB proteins from *Burkholderia pseudomallei* (*Bp*), *B. thailandensis* (*Bt*), *Pseudomonas aeruginosa* (*Pa*), and *Chlamydia psittaci* (*Cp*) have been assayed to find inhibitors. Interestingly, Rose Bengal (4,5,6,7-tetrachloro-2',4',5',7'-tetraiodofluorescein) was turned out to be an inhibitor of three KdsBs (*Bp*KdsB, *Bt*KdsB, and *Pa*KdsB) with promising IC<sub>50</sub> values and increased thermostability. The inhibitory enzyme kinetics of Rose Bengal revealed that it is competitive with 2-keto-3-deoxy-manno-octulosonic acid (KDO) but non-competitive against cytidine 5'-triphosphate (CTP). Induced-fit docking analysis of *Pa*KdsB revealed that Arg160 and Arg185 together with other interactions in the substrate binding site seemed to play an important role in binding with Rose Bengal. We suggest that Rose Bengal can be used as the scaffold to develop potential antibiotics.

### ARTICLE HISTORY

Received 8 January 2020  
Revised 16 March 2020  
Accepted 30 March 2020

### KEYWORDS

CMP-2-keto-3-deoxy-D-manno-octulosonic acid biosynthesis pathway; 2-keto-3-deoxy-D-manno-octulosonate cytidyltransferase (KdsB); melioidosis; multi-drug resistance; Rose Bengal

### Introduction

The 2-keto-3-deoxy-manno-octulosonic acid (KDO) which is an eight carbon acidic sugar composing the lipopolysaccharide (LPS) has a vital role in keeping outer membrane (OM) integrity and viability of most Gram-negative bacteria<sup>1,2</sup>. The KDO biosynthesis pathway consists of six enzymes: Ribose-5-phosphate isomerase (RpiA)<sup>3</sup>; D-arabinose-5-phosphate isomerase (KpsF)<sup>4</sup>; KDO-8-phosphate synthase (KdsA)<sup>5</sup>; KDO-8-phosphate phosphatase (Yrbl)<sup>6</sup>; 2-keto-3-deoxy-D-manno-octulosonate cytidyltransferase (KdsB), and glycosyltransferase (WaaA) which transfers the KDO from cytidine 5'-monophospho-2-keto-3-deoxy-manno-octulosonic acid (CMP-KDO) to the lipid A<sup>7</sup>. In LPS, KDO molecules are important to connect the core oligosaccharide with the lipid A<sup>8–10</sup>. Therefore, the KDO biosynthesis pathway has been considered as the potential target for the advanced antibiotics against Gram-negative bacteria<sup>1,11</sup>.

*Burkholderia pseudomallei* (*Bp*) is the etiologic agent of a serious and often fatal syndrome known as melioidosis<sup>12–15</sup>. Melioidosis features various symptoms like a self-limiting abscess, sepsis, necrotising pneumonia, osteomyelitis, and dissemination to the solid organs and brain<sup>15–19</sup>. On the other hand, *Burkholderia thailandensis* (*Bt*) which is highly relevant to *Bp*<sup>20</sup> is reported to cause sporadic human disease even if *Bt* has been informed as non-pathogenic bacteria<sup>21,22</sup>. A similar but differently classified microbe, *Pseudomonas aeruginosa* (*Pa*), is an opportunistic pathogen and common Gram-negative bacillus in and around people<sup>23</sup>. Almost all infection cases of *Pa* can progress through nullifying host defence systems. *P. aeruginosa* infection can occur to patients who have general immunosuppression because of HIVs<sup>24–26</sup>. Also,



*Pa* can cause various disease in our whole body, as secondary consequent results of the collapse of normal physiological function such as bacteraemia after severe burn, chronic lung infection in cystic fibrosis and acute ulcerative keratitis in soft contact lenses users<sup>23</sup>. In the same context, *Pa* is one of the major pathogens causing hospital-acquired infections<sup>27</sup>.

Three Gram-negative bacteria above have already been reported for their antibiotics resistance. Acquired or intrinsic resistant *Burkholderia* species for primary antibiotic treatment has been identified<sup>28–30</sup>. Moreover, *Pa* is resistant to an extensive range of antibiotics and can advance resistance to antimicrobials which are frequently used through mutations in genes or by the acquisition of resistant factors<sup>27</sup>. To overcome these resistant bacteria, we targeted KdsB involved in KDO biosynthesis from four pathogenic microbes (*Bp*, *Bt*, *Pa*, and *Chlamydia psittaci* (*Cp*)) to find potent antibiotic candidate molecules.

### Materials and methods

#### Preparation of protein native KdsB proteins

The two of four KdsB genes (*BpkdsB* and *BtkdsB*) (NCBI reference sequence: NC\_006350.1; NC\_007651.1) coding for the proteins (*Bp*KdsB and *Bt*KdsB) were amplified by using of primers and ligated into the amplified expression vector pB<sub>2</sub> by way of ligation-independent cloning (LIC) method. The rest of genes (*CpkdsB* and *PakdsB*) (NCBI reference sequence: WP\_006343263.1; WP\_003106922.1) coding for the proteins (*Cp*KdsB and *Pa*KdsB) were inserted in the pBT<sub>7</sub> plasmid DNA (pDNA) and gained from Bioneer (Daejeon, South Korea). To express the proteins, we

**CONTACT** Dong Hae Shin  [dhshin55@ewha.ac.kr](mailto:dhshin55@ewha.ac.kr)  Department of Pharmacy, Ewha Woman's University, Seoul 03760, Republic of Korea

 Supplemental data for this article can be accessed [here](#).

© 2020 The Author(s). Published by Informa UK Limited, trading as Taylor & Francis Group.

This is an Open Access article distributed under the terms of the Creative Commons Attribution License (<http://creativecommons.org/licenses/by/4.0/>), which permits unrestricted use, distribution, and reproduction in any medium, provided the original work is properly cited.

transformed pDNAs into *Escherichia coli* (*E. coli*) BL21 (DE3). Transformed *E. coli* cells were incubated on Luria-Bertani (LB) agar plates. Several colonies were chosen and grown in test tubes with a cap to determine the condition for culturing in bulk. In the process, a cell stock was prepared and frozen. The mass culture proceeded at 310 K with shaking. As the absorbance at 600 nm of broth reached 0.6–0.8, isopropyl- $\beta$ -D-1-thiogalactopyranoside was put for expression of KdsB proteins (KdsBs). The cultures of *BpKdsB*, *BtKdsB*, and *CpKdsB* were incubated at 298 K for 16 h and the culture of *PaKdsB* was incubated at 310 K for 3 h. The expressed proteins contained non-cleavage N-terminal His<sub>6</sub>-tags followed by five glycines in *BpKdsB*, *BtKdsB* (MHHHHH GGGGG) and eight amino acids in *CpKdsB*, *PaKdsB* EFSQQDSD (MHHHHH EFSQQDSD). To collect cells, we centrifuged the culture fluid with a high-speed refrigerated centrifuge at 7650 $\times$ g (6500 rev min<sup>-1</sup>) for 10 min at 277 K. The cultured cell pellet was suspended and fragmented using a Digital Sonifier 450 (Branson Ultrasonics Co., Danbury, CT). Cell debris was pelleted by centrifugation. Using a HisTrap column (GE Healthcare, Piscataway, NJ), Affinity chromatography was done with the supernatant on an ÄKTA explorer system (GE Healthcare, Piscataway, NJ). Ion-exchange chromatography has been done as the secondary purifications using a 5 ml Hi-Trap Q column (GE Healthcare, Piscataway, NJ). The mobile phase buffer of the Q column and the concentration of sodium chloride at which proteins were eluted for each KdsB are organised in Table 1. The purified native proteins were concentrated to adequate concentration for using in the assay. The purity of proteins was at least 95% as considered by SDS/PAGE.

### Chemical screening with a malachite green assay method

The screening of about two hundred chemical compounds (Supplementary Table 1) was performed with a malachite green assay method which is a photometric method<sup>31</sup>. The principle of this method is: when KdsBs transfer the cytidine 5'-monophosphate (CMP) moiety from cytidine 5'-triphosphate (CTP) to KDO, CMP-KDO, and pyrophosphate (PPi) are produced. PPi was decomposed into two phosphates by inorganic pyrophosphatase (IPP) and phosphates were measured by the malachite green method. CTP and KDO purchased from Sigma (St. Louis, MO) were used as a real substrate. A colour reagent of the malachite green method for phosphate detection was a mixture of ammonium molybdate ((NH<sub>4</sub>)<sub>6</sub>Mo<sub>7</sub>O<sub>24</sub>), malachite green solution and Tween 20 in the ratio 1:3:0.1. The mixture was filtered through a 0.20  $\mu$ m PVDF syringe filter (Younginfrontier Inc., Seoul, Republic of Korea) and allowed to stand at room temperature (RT) for 1 h before use. The probability of inhibitory function of each chemical was investigated by detecting the difference in absorbance between the reaction mixtures with and without KdsBs.

Table 1. The Q column experiments.

Protein	Size <sup>a</sup> (kDa)	Buffer <sup>b</sup>	NaCl <sup>c</sup> (M)
<i>BpKdsB</i>	30	20 mM Tris-HCl pH 8.5	0.24
<i>BtKdsB</i>	28.5	20 mM Tris-HCl pH 8.0	0.66
<i>CpKdsB</i>	30.4	20 mM Tris-HCl pH 7.5	N/A <sup>d</sup>
<i>PaKdsB</i>	29.5	20 mM Bis-Tris pH 7.0	0.27

<sup>a</sup>The molecular weight of the proteins on SDS-PAGE.

<sup>b</sup>The equilibration buffer conditions.

<sup>c</sup>The NaCl concentration at elution.

<sup>d</sup>*CpKdsB* was done only with the affinity chromatography.

### Enzyme kinetics of KdsBs

The malachite green assay method<sup>31</sup> was used to study steady-state kinetics of KdsBs (*BpKdsB*, *BtKdsB*, and *PaKdsB*). For the kinetic studies, reaction mixtures including 5 mM Tris-HCl (pH 7.5), 10 mM MgCl<sub>2</sub>, 0.04 unit IPP, and 0.01 mg ml<sup>-1</sup> KdsBs with different concentrations of CTP (0.00098–0.25 mM) at the constant concentration of KDO (0.25 mM) and with different concentrations of KDO (0.000195–1 mM) at the constant concentration of CTP (0.1 mM) were used. After incubation at RT for an hour, 40  $\mu$ l of reaction mixtures were mixed with the malachite reagent (160  $\mu$ l). The mixtures were left for 10 min to develop the colour. The standard curve was plotted and devices were used as in previous studies<sup>32</sup>.

### IC<sub>50</sub> value of Rose Bengal

The malachite green assay method<sup>31</sup> was also used to study the dose-dependent inhibitory effect of Rose Bengal (4,5,6,7-tetrachloro-2',4',5',7'-tetraiodofluorescein) purchased from Tokyo Chemical Industry (Tokyo, Japan). The 40  $\mu$ l of reaction mixtures containing 5 mM Tris-HCl (pH 7.5), 10 mM MgCl<sub>2</sub>, and 0.01 mg ml<sup>-1</sup> KdsBs with different concentrations of Rose Bengal (0.098–100  $\mu$ M) were incubated at RT for an hour. The reaction mixtures lacking KdsBs with the same concentration of Rose Bengal used as above were also incubated at RT for an hour and measured as blanks. The reaction was initiated by adding 0.25 mM KDO and 0.1 mM CTP and stood for an hour. After incubation, 160  $\mu$ l of the same malachite reagent used above was added and left for 10 min. The absorbance was measured at 620 nm using the microplate spectrophotometer (Spectramax 190, Molecular Devices Corporation, Sunnyvale, CA). Rose Bengal is a photoreactive compound with its absorbance peaks at 258 nm, 519 nm, and 562 nm<sup>33</sup>. Therefore, the measurement wavelength of the malachite green assay is not influenced by Rose Bengal. The percentage reactivity (%Reactivity) was calculated depending on the difference in absorbance of whether or not KdsBs was present in the reaction mixture. The IC<sub>50</sub> values of Rose Bengal against KdsBs were calculated by a nonlinear regression analysis using GraphPad Prism 8.3.0 (GraphPad Software, La Jolla, CA).

### Inhibitory enzyme kinetics

To specify the binding site of compounds for the induced fit docking, we studied the inhibitory enzyme kinetics using malachite green assay. Reaction mixtures including 5 mM Tris-HCl (pH 7.5), 10 mM MgCl<sub>2</sub>, 0.04 unit IPP, 0.01 mg ml<sup>-1</sup> *PaKdsB*, and 14.66  $\mu$ M Rose Bengal with different concentrations of CTP (0.00098–0.25 mM) at the constant concentration of KDO (0.25 mM) and with different concentrations of KDO (0.000195–2.5 mM) at the constant concentration of CTP (0.1 mM) were used.

### Sample preparation and circular dichroism (CD) spectroscopy

Native *BpKdsB* (0.2 mg ml<sup>-1</sup>) and *BpKdsB* co-incubated at 4 °C with Rose Bengal in a mole ratio of 1:20 (protein:Rose Bengal) were ready for *T<sub>m</sub>* value measurement. The CD sample buffer conditions were 20 mM Tris pH 8.5. CD measurements were taken with a J-1500 Circular Dichroism Spectrophotometer (JASCO Co., Mary's Court, Easton, MD) equipped with a computer-controlled water bath, and samples were placed in a Rectangular Quartz Cell of 1 mm optical path length. The thermal denaturation was

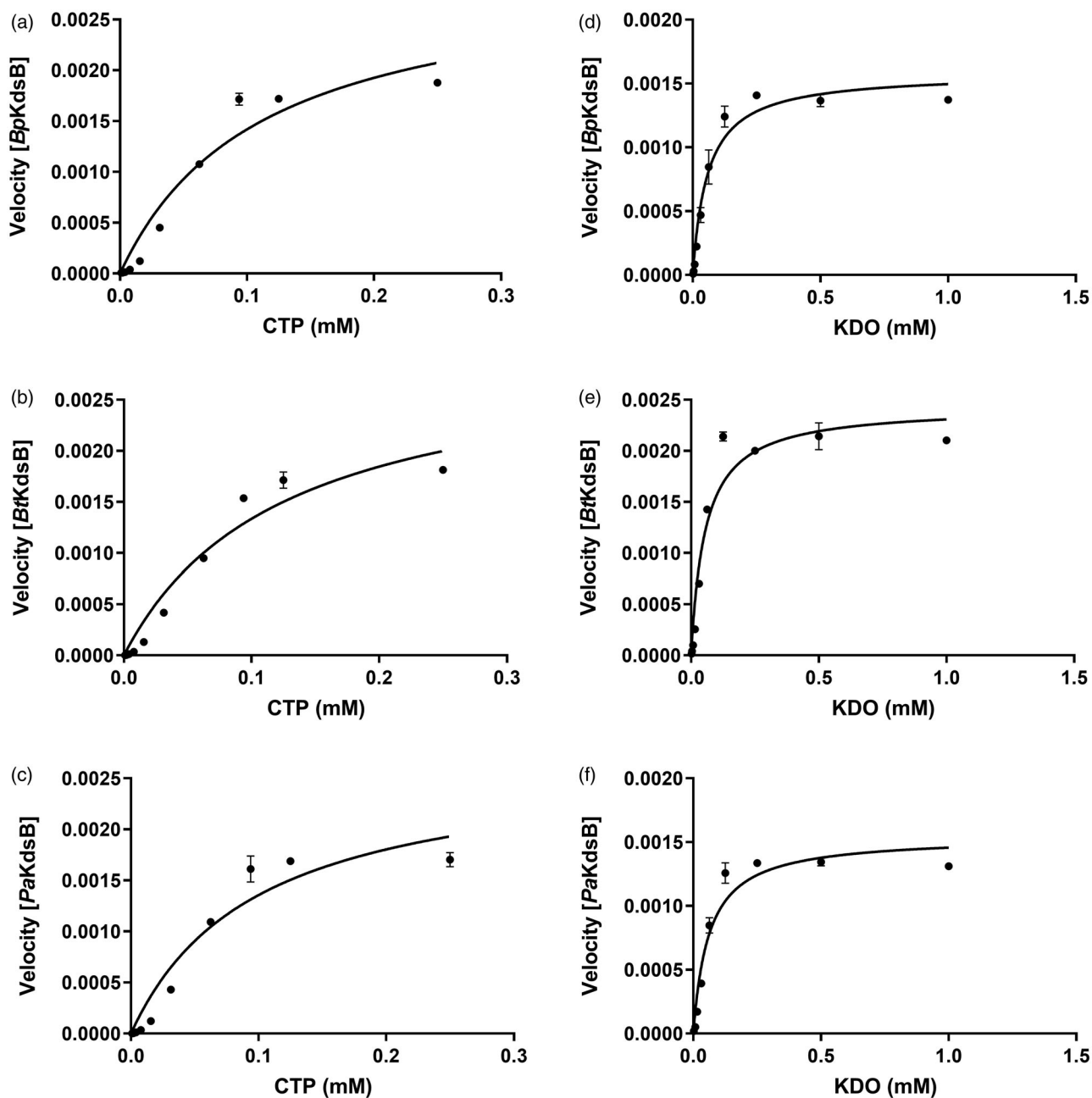


**Figure 1.** The specific enzyme activities of *BpKdsB*, *BtKdsB*, and *PaKdsB*. The enzyme activities with (a–c) different concentrations of CTP in the presence of 0.25 mM KDO and (d–f) different concentrations of KDO in the presence of 0.1 mM CTP.

observed at 222 nm from 25 °C to 95 °C at 1 °C min<sup>-1</sup> rate. Data analysis and display were done using Spectra Manager Version 2, Thermal Denaturation Multi Analysis version 2.1.0.1 software.

To ascertain the thermostability of KdsBs with Rose Bengal, three native KdsBs (*BpKdsB*, *BtKdsB*, and *PaKdsB*) (1 mg ml<sup>-1</sup>) and KdsBs bound with Rose Bengal (0.625 mM for *BpKdsB*, 1.25 mM for *BtKdsB*, and 2.5 mM for *PaKdsB*) were prepared. All samples were heated at 80 °C for 5 min and Rose Bengal bound samples were also heated at 100 °C for 5 min.

#### Ligand preparation, target preparation, and induced-fit docking

All the docking and scoring calculations were performed using the Schrödinger software suite (Maestro, version 11.8.012) against the substrate and nucleotide binding sites of *PaKdsB*. The SDF file

of Rose Bengal was got from the PubChem database. The file was imported into Maestro and prepared for docking using ligand preparation. The atomic coordinates of the crystal structure of *PaKdsB* (PDB ID: 4XWI) were saved from the Protein Data Bank and prepared by removing all solvent and adding hydrogens and minimal minimisation using Protein Preparation Wizard. Ioniser was used to generate an ionised state of Rose Bengal at the target pH 7.5 ± 2.0. The input for an induced-fit docking is the prepared low-energy ligand forms. The induced-fit docking protocol<sup>34</sup> was worked on the graphical user interface, Maestro 11.8.012 linked with the Schrödinger software. Receptor sampling and refinement were conducted for residues within 5.0 Å of each ligand and for each ligand–protein complex. With Prime<sup>35</sup>, a side-chain sampling and prediction module, as well as the backbone of the target protein, were minimised in energy. A total of induced-fit

receptor conformations were generated for Rose Bengal. Finally, the ligand poses were scored using a combination of Prime and Glide Score scoring functions<sup>36</sup>.

## Results

### Chemical screening with a malachite green assay method

The enzyme activity of KdsBs was confirmed and the chemical screening of about 200 compounds was done with the malachite green assay method<sup>31</sup>. It is a fast, reproducible, colorimetric method for measuring inorganic free phosphate in aqueous solutions. Hence, the assay offered great ease for exploring potent inhibitors against KdsBs. A list of compounds' names is provided as Supplementary Table 1 in the Supplementary Materials. As a result of the screening, one potent inhibitor, Rose Bengal, blocking three KdsBs (*BpKdsB*, *BtKdsB*, and *PaKdsB*) was detected. However, no hit was found against *CpKdsB*.

### Enzyme kinetics of three KdsBs

To determine the kinetic parameters for KDO and CTP, enzyme assays were performed with various concentrations of CTP at a constant KDO concentration (0.25 mM) and with various concentrations of KDO at a constant CTP concentration (0.1 mM). The graphs of the velocities versus concentrations of KDO and CTP are shown in Figure 1. The graphs indicated that the maximum velocity was obtained at 0.1 mM CTP in the presence of 0.25 mM KDO and at 0.25 mM KDO in the presence of 0.1 mM CTP. The kinetic parameter data of CTP and KDO at the steady-state are organized in Table 2.

### The IC<sub>50</sub> value of Rose Bengal

The inhibitory effect of Rose Bengal against KdsBs was found through a chemical screening with the malachite green assay method. The dose-dependent inhibitory effect of Rose Bengal was estimated at the saturated substrate concentrations (0.1 mM CTP and 0.25 mM KDO). The results were plotted as log inhibitor concentration versus percentage reactivity of absorbance (Figure 2). The IC<sub>50</sub> value determined from the dose-dependent inhibitory curve of Rose Bengal: *BpKdsB* was 5.31 μM; *BtKdsB* was 7.24 μM; *PaKdsB* was 14.66 μM.

### T<sub>m</sub> value CD-ORD and thermostability

The binding effect of Rose Bengal was tested with the measurement of the T<sub>m</sub> values of native and complex *BpKdsB*. The T<sub>m</sub> value of native *BpKdsB* was 76.8 °C. Interestingly, that of Rose Bengal bound form was not measurable because *BpKdsB* became heat stable and thus did not denatured at 100 °C. The similar effect on thermostability increased by Rose Bengal was also found in *BtKdsB* and *PaKdsB*. The thermal denaturation test showed that three native KdsBs were all precipitated at around 80 °C. However, the three KdsBs treated with Rose Bengal with their full inhibitory concentration were all stable at 100 °C for 5 min. Therefore, the increased thermostability of KdsBs could be the sign of compound binding.

**Table 2.** The KdsBs kinetics parameters.

KdsBs	CTP		KDO	
	$k_{cat}$ (min <sup>-1</sup> )	$K_m$ (mM)	$k_{cat}$ (min <sup>-1</sup> )	$K_m$ (mM)
<i>BpKdsB</i>	9.986 ± 1.322	0.1111 ± 0.031	5.278 ± 0.223	0.059 ± 0.009
<i>BtKdsB</i>	8.540 ± 1.156	0.1239 ± 0.034	6.961 ± 0.372	0.056 ± 0.011
<i>PaKdsB</i>	7.911 ± 1.104	0.0983 ± 0.030	4.547 ± 0.230	0.061 ± 0.011

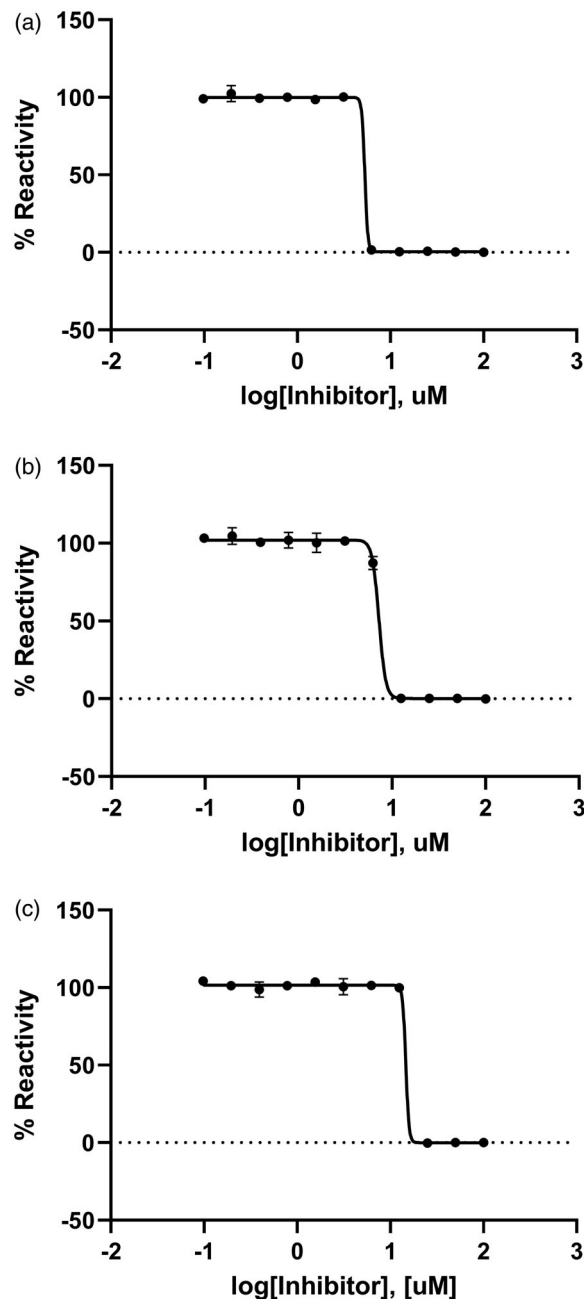


**Figure 2.** A dose-dependent inhibitory curve for the inhibition of (a) *BpKdsB*, (b) *BtKdsB*, and (c) *PaKdsB* by Rose Bengal.

### Inhibitory enzyme kinetics and docking

According to the inhibitory enzyme kinetics, Rose Bengal was turned out to be a competitive inhibitor against KDO in *PaKdsB* (Figure 3). To deduce the binding modes of Rose Bengal with KdsBs in the atomic level, an in-depth theoretical investigation with an induced-fit docking study using the Schrödinger programme was carried out. The crystal structure of *PaKdsB*

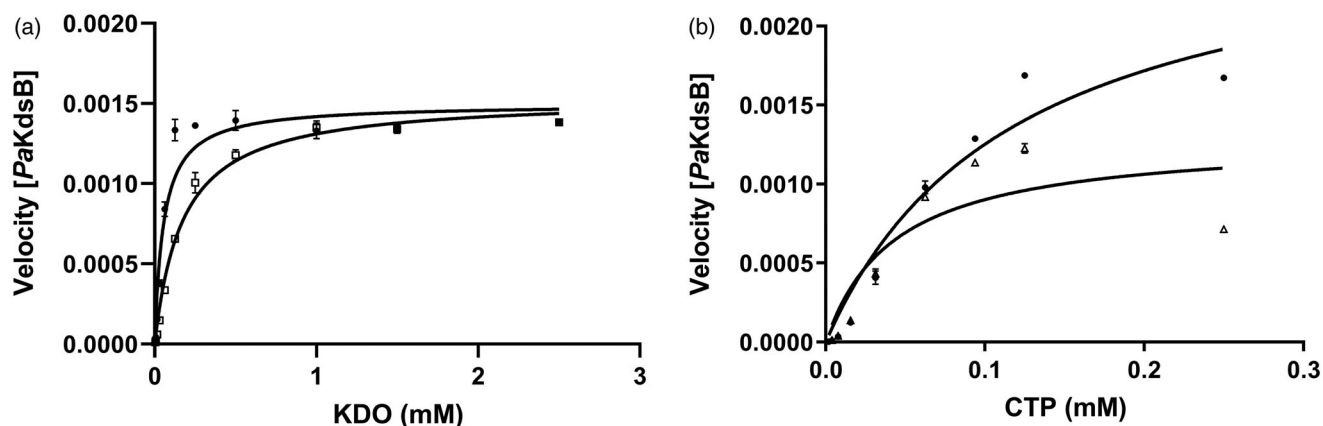


**Figure 3.** The inhibitory enzyme kinetics of KdsB from *Pseudomonas aeruginosa* (*PaKdsB*). The enzyme activities with (a) different concentrations of CTP in the presence of 0.25 mM KDO and (b) different concentrations of KDO in the presence of 0.1 mM CTP. Filled circles represent the inhibitory enzyme kinetics with DMSO and squares for with 14.66  $\mu$ M Rose Bengal in (a). Filled circles represent the inhibitory enzyme kinetics with DMSO and triangles for with 14.66  $\mu$ M Rose Bengal in (b).

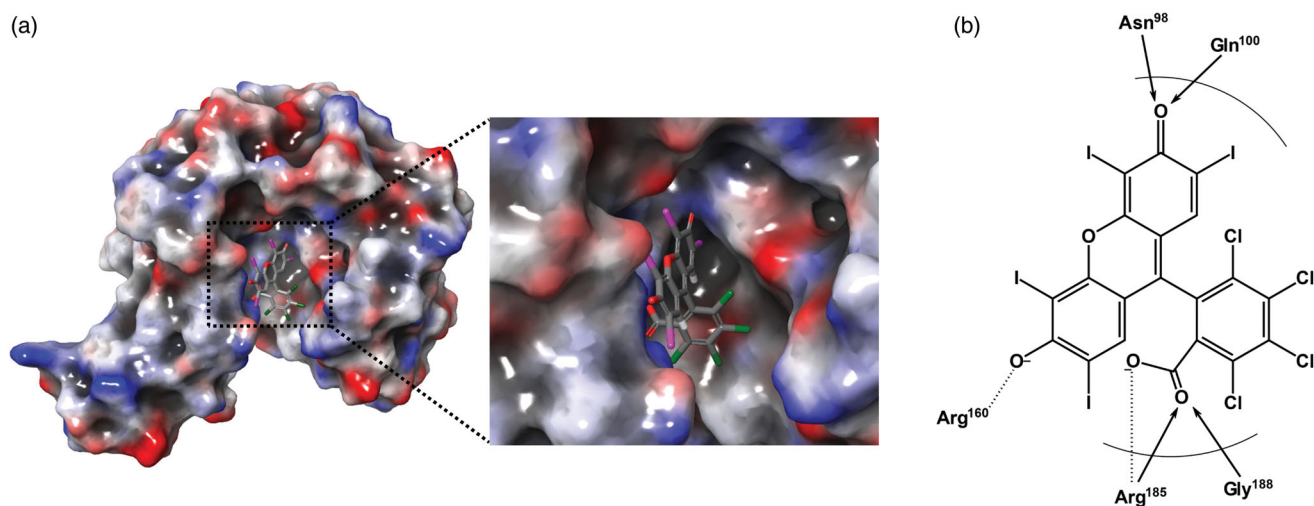


**Figure 4.** A predicted docking mode of Rose Bengal in the catalytic site of *PaKdsB*. (a) The docking pose of Rose Bengal was depicted on the electrostatic surface potential of *PaKdsB* (red, negative; blue, positive; white, uncharged). The enlarged view of the active site docked with Rose Bengal was depicted with dot lines. In addition, (b) a 2D schematic representation of the docked Rose Bengal with *PaKdsB* was drawn. Figures were created with Maestro v11.5.011. The dot line represents the ion interaction by Arg160 and Arg185 and the arrow represents the hydrogen bond interaction with Asn95, Gln100, and Gly188.

deposited in the Protein Data Bank was retrieved and docked with Rose Bengal to predict its binding mode. Top-ranked structures with the highest Glide  $g$ -scores from the induced-fit docking results were surveyed. The top model was obtained among docked models in the substrate binding pocket and had the  $g$ -score of  $-7.19$ . The  $g$ -score of the best model docked in the nucleotide binding site was  $-5.62$ . The predicted complex structure and 2D schematic representation of the top model are illustrated in Figure 4.

## Discussion

All of the four KdsBs from pathogenic bacteria were well expressed. The sequence alignment showed that their overall sequence identities against *Pa* were roughly from 38 to 55%. Therefore, their molecular behaviours are expected to be similar. The malachite assay of four KdsBs was carried out with a homemade chemical library composed of two hundred compounds. All of the chemicals excluding Rose Bengal did not show any inhibitory tendency against four KdsBs. Interestingly, inhibitory activity of Rose Bengal appeared against the three KdsBs (*BpKdsB*, *BtKdsB*,

and *PaKdsB*). However, its inhibitory effect is negligible against *CpKdsB*.  $T_m$  value measurement through CD spectrometry was performed to independently confirm the binding of Rose Bengal with *BpKdsB*. Intriguingly, a  $T_m$  value of *BpKdsB* complexed with Rose Bengal could not be obtained because the thermostability of the complex was increased. Therefore, a thermostability test was done using a hit block and proved that *BpKdsB* bound with Rose Bengal became thermostable at 100 °C for 5 min. In contrast, its native form was precipitated at 80 °C for 5 min. Therefore, the thermostability test could be an independent method to prove the binding capability of chemicals in the case of the KdsB family. The same result was obtained with *BtKdsB* and *PaKdsB*.

Enzyme kinetics was performed with three KdsBs to identify the inhibitory effect of Rose Bengal (Table 2, Figure 1) and its  $IC_{50}$  values (Figure 2). The  $IC_{50}$  values are 5.31  $\mu$ M for *BpKdsB*, 7.24  $\mu$ M for *BtKdsB*, and 14.66  $\mu$ M for *PaKdsB*. Therefore, Rose Bengal is a quite good candidate for further development as potential antibiotics. In order to understand the inhibition mechanism of Rose Bengal, the enzyme activity of *PaKdsB* was determined as a function of KDO concentration in the absence or in the presence of Rose Bengal. The plot obtained reflected typical competitive inhibition kinetics (Figure 3(a)). On the other hand, a non-competitive

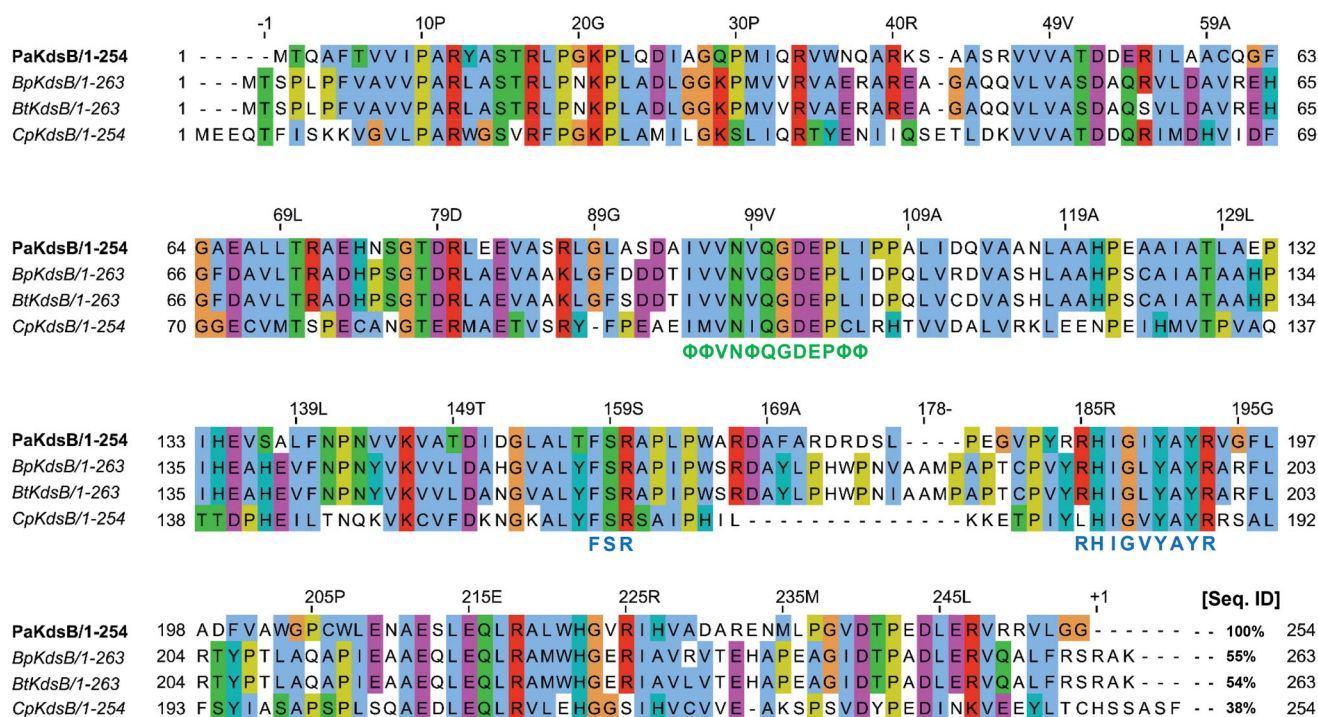


**Figure 5.** Sequence alignment of PaKdsB with the rest of three KdsBs. Pa: *Pseudomonas aeruginosa*; Bp: *Burkholderia pseudomallei*; Bt: *Burkholderia thailandensis*; Cp: *Chlamydia psittaci*. The highly conserved motifs were indicated. Green letters mean the nucleotide binding motif in the catalytic cavity. Blue letters mean the substrate binding motifs. The % sequence identity was calculated with PaKdsB as a reference sequence. The consensus amino acid ID coloured according to the Clustal X colour scheme provided by the Jalview program<sup>37</sup>.

inhibition mode of binding was exhibited with respect to CTP (Figure 3(b)). The result indicated that Rose Bengal competitively occupies the substrate binding site rather than the nucleotide binding site. For the understanding of the inhibitory activity of Rose Bengal against PaKdsB in the atomic level, an induced-fit molecular docking experiment against the substrate and nucleotide binding sites of PaKdsB using Glide scoring and docking methodology was executed. The Glide *g*-score obtained from the docking on the substrate binding site was  $-7.19$  and that from the nucleotide binding site was  $-5.62$ , respectively. The better Glide *g*-score from the substrate binding site implies that the affinity of Rose Bengal is greater at the substrate binding site. In the top model, Rose Bengal is well docked in the substrate pocket of PaKdsB. There are major three interactions between Rose Bengal and PaKdsB (Figure 4). At first, there are two hydrogen bonds between the 6-oxo moiety of Rose Bengal and two residues, Asn98 and Gln100, on the nucleotide binding motif,  $^{95}\Phi\text{VNV}\Phi\text{QGD}\Phi\text{E}\Phi\text{P}\Phi\text{P}\Phi^{106}$  (Figure 5). Second, there is one salt bridge between the 3-hydroxyl moiety of Rose Bengal and Arg160 on the substrate binding motif,  $^{158}\text{FSR}^{160}$ . Third, there are also one salt bridge and one hydrogen bond between the benzoic acid moiety of Rose Bengal and Arg185 on another substrate binding motif,  $^{185}\text{RHIGVYAYR}^{193}$ . As shown in the sequence alignment, the Rose Bengal binding motifs found in PaKdsB are also conserved in the other two KdsBs. The similar experimental result of the two KdsBs can be explained by the sequence homology. However, CpKdsB shares low sequence homology and some of its residues in the highly conserved motifs are divergent (Figure 5). Specially, the last interaction operated by Arg185 is not possible in the case of CpKdsB. The conserved arginine on this motif is replaced by leucine in CpKdsB. The overall result indicated that Rose Bengal tightly binds to BpKdsB, BtKdsB, and PaKdsB. Considering the increased thermostability of the three KdsBs, the binding of Rose Bengal would trigger a conformational change. The structure of

PaKdsB indicates that its valley-like centre is open and lined up by two domains (Figure 4(a)). Rose Bengal seems to induce a closed conformation of PaKdsB, which may confer the resistance of PaKdsB against thermal deactivation.

Rose Bengal is an organic anion dye that has been clinically used for decades and has been used to assess eye surface epithelium damage of eye surface disease<sup>38</sup>. Also, it is a water-soluble photosensitizer with a distinctive wine colour<sup>39</sup>. It is well known that singlet-oxygen production of Rose Bengal after exposure with 300–600 nm radiation increases the antibacterial effect<sup>40–43</sup>. Besides, Rose Bengal was reported as a potent inhibitor of the DNA dependent RNA polymerase of *E. coli* without photooxidation<sup>44</sup>. On the other hand, Rose Bengal can be a possible choice in the treatment of cancer. For instance, PV-10 (injective Rose Bengal developed by Provectus) was found to cause visible therapeutic responses in melanoma patients<sup>45</sup>. Since 2016, PV-10 has been performed as a single treatment for locally advanced cutaneous melanoma patients who participated in phase 3 of clinical research (clinical trials ID NCT02288897). Rose Bengal also has been shown to prevent the growth and spread of ovarian cancer, and to induce the apoptotic cell death of the cancer cells *in vitro*<sup>46</sup>. Therefore, Rose Bengal possesses various beneficial functions against human diseases. This study also suggests a potential usage of Rose Bengal as an antibiotic targeting three KdsBs. Unfortunately, however, the antibiotic effect of Rose Bengal against Gram-negative species was reported to be inefficient due to the presence of LPS obstructing the absorbance of charged compounds<sup>47,48</sup>. Therefore, photosensitising techniques to induce the antibiotic property of Rose Bengal by producing reactive oxygen species have been employed.

Nevertheless, the discovery of the direct inactivation of three KdsBs by Rose Bengal was informative and thus can be applied to enhance the antibiotic property of Rose Bengal. Specially, we propose the combined usage of Rose Bengal with polymyxin B

nonapeptide (PMBN). PMBN has been suggested to increase the permeability of Rose Bengal into OMs of Gram-negative bacteria<sup>49</sup>. Since Rose Bengal-mediated photoinactivation against multidrug resistance *Pa* has been known<sup>50</sup>, a combined therapy increasing absorption of Rose Bengal with antimicrobial peptides should be tested<sup>51</sup>. All the properties of Rose Bengal can be applied and developed to design an anti-melioidosis agent. The crystallisation of the three KdsBs complexed with Rose Bengal is going on to determine the complex structures with X-ray crystallography.

## Conclusions

KdsB is one of the key enzymes in the CMP-KDO biosynthesis pathway. Two researches to develop antibiotics targeting this enzyme were reported. One targeted KdsB from *E. coli*<sup>52</sup> and the other for *Agrobacterium tumefaciens* and *Aeromonas salmonicida*<sup>53</sup>. However, no further study has been followed. This study discovered the probability of Rose Bengal as a potential antibiotic agent targeting KdsB. Rose Bengal has beneficiary roles in other human diseases and possesses a photodynamic property. Considering a severe fatality of melioidosis caused by *Bp* and multidrug-resistance of *Pa*, the development of Rose Bengal and its derivatives with various combined therapies may provide a promising way to overcome these disease.

## Disclosure statement

No potential conflict of interest was reported by the author(s).

## Funding

This work was supported by the Basic Science Research Programs, 2018R1D1A1B07050781 to DHS and 2018R1D1A1B07050942 to M-SK, funded by the National Research Foundation of Korea grant granted by the Ministry of Education, Science and Technology, Republic of Korea (MEST).

## ORCID

Dong Hae Shin  <https://orcid.org/0000-0002-2205-1453>

## References

- Smyth KM, Marchant A. Conservation of the 2-keto-3-deoxy-manno-octulosonic acid (Kdo) biosynthesis pathway between plants and bacteria. *Carbohydr Res* 2013;380:70–5.
- Mamat U, Schmidt H, Munoz E, et al. WaaA of the hyperthermophilic bacterium *Aquifex aeolicus* is a monofunctional 3-deoxy-D-manno-oct-2-ulosonic acid transferase involved in lipopolysaccharide biosynthesis. *J Biol Chem* 2009;284:22248–62.
- Hove-Jensen B, Maigaard M. *Escherichia coli* rpiA gene encoding ribose phosphate isomerase A. *J Bacteriol* 1993;175:5628–35.
- Meredith TC, Woodard RW. *Escherichia coli* YrbH is a D-arabinose 5-phosphate isomerase. *J Biol Chem* 2003;278:32771–7.
- Radaev S, Dastidar P, Patel M, et al. Structure and mechanism of 3-deoxy-D-manno-octulosonate 8-phosphate synthase. *J Biol Chem* 2000;275:9476–84.
- Park J, Lee D, Kim MS, et al. A preliminary X-ray study of 3-deoxy-D-manno-oct-2-ulosonic acid 8-phosphate phosphatase (YrbI) from *Burkholderia pseudomallei*. *Acta Crystallogr F Struct Biol Commun* 2015;71:790–3.
- Belunis CJ, Raetz CR. Biosynthesis of endotoxins. Purification and catalytic properties of 3-deoxy-D-manno-octulosonic acid transferase from *Escherichia coli*. *J Biol Chem* 1992;267:9988–97.
- Hammond SM, Claesson A, Jansson A, et al. A new class of synthetic antibacterials acting on lipopolysaccharide biosynthesis. *Nature* 1987;327:730–2.
- Goldman R, Kohlbrenner W, Lartey P, Pernet A. Antibacterial agents specifically inhibiting lipopolysaccharide synthesis. *Nature* 1987;329:162–4.
- Claesson A, Jansson AM, Pring BG, et al. Design and synthesis of peptide derivatives of a 3-deoxy-D-manno-2-octulosonic acid (KDO) analogue as novel antibacterial agents acting upon lipopolysaccharide biosynthesis. *J Med Chem* 1987;30:2309–13.
- Rick D, Osborn MJ. Isolation of a mutant of *Salmonella typhimurium* dependent on D-arabinose-5-phosphate for growth and synthesis of 3-deoxy-D-mannoctulosonate (ketodeoxyoctonate). *Proc Natl Acad Sci USA* 1972;69:3756–60.
- Cheng AC, Currie BJ. Melioidosis: epidemiology, pathophysiology, and management. *Clin Microbiol Rev* 2005;18:383–416.
- Limmathurotsakul D, Peacock SJ. Melioidosis: a clinical overview. *Brit Med Bull* 2011;99:125–39.
- Peacock SJ. Melioidosis. *Curr Opin Infect Dis* 2006;19:421–8.
- Wiersinga WJ, Currie BJ, Peacock SJ. Melioidosis. *N Engl J Med* 2012;367:1035–44.
- Bartley PP, Pender MP, Woods ML 2nd, Walker D, et al. Spinal cord disease due to melioidosis. *Trans R Soc Trop Med Hyg* 1999;93:175–6.
- Caldera AS, Kumanan T, Corea E. A rare cause of septic arthritis: melioidosis. *Trop Doct* 2013;43:164–6.
- Jane L, Crowe A, Daffy J, Gock H. *Burkholderia pseudomallei* osteomyelitis: an unusual cause of fever in a returned traveller. *Aust Med J* 2012;5:141–3.
- McLeod C, Morris PS, Bauert PA, et al. Clinical presentation and medical management of melioidosis in children: a 24-year prospective study in the Northern Territory of Australia and review of the literature. *Clin Infect Dis* 2015;60:21–6.
- Ngamdee W, Tandhavanant S, Wikraiphath C, et al. Competition between *Burkholderia pseudomallei* and *B. thailandensis*. *BMC Microbiol* 2015;15:56.
- Glass MB, Gee JE, Steigerwalt AG, et al. Pneumonia and septicemia caused by *Burkholderia thailandensis* in the United States. *J Clin Microbiol* 2006;44:4601–4.
- Lertpatanasuwan N, Sermsri K, Petkaseam A, et al. Arabinose-positive *Burkholderia pseudomallei* infection in humans: case report. *Clin Infect Dis* 1999;28:927–8.
- Lyczak JB, Cannon CL, Pier GB. Establishment of *Pseudomonas aeruginosa* infection: lessons from a versatile opportunist. *Microbes Infect* 2000;2:1051–60.
- Franzetti F, Cernuschi M, Esposito R, Moroni M. *Pseudomonas* infections in patients with AIDS and AIDS-related complex. *J Intern Med* 1992;231:437–43.
- Kielhofner M, Atmar RL, Hamill RJ, Musher DM. Life-threatening *Pseudomonas aeruginosa* infections in patients with human immunodeficiency virus infection. *Clin Infect Dis* 1992;14:403–11.

26. Bendig JW, Kyle PW, Giangrande PL, et al. Two neutropenic patients with multiple resistant *Pseudomonas aeruginosa* septicaemia treated with ciprofloxacin. *J R Soc Med* 1987;80:316–7.
27. Ruiz-Garbajosa P, Cantón R. Epidemiology of antibiotic resistance in *Pseudomonas aeruginosa*. Implications for empiric and definitive therapy. *Rev Esp Quimioter* 2017;30:8–12.
28. Boucher HW, Talbot GH, Bradley JS, et al. Bad bugs, no drugs: no ESKAPE! An update from the Infectious Diseases Society of America. *Clin Infect Dis* 2009;48:1–12.
29. Michael CA, Dominey-Howes D, Labbate M. The antimicrobial resistance crisis: causes, consequences, and management. *Front Public Health* 2014;2:145.
30. Yi H, Kim K, Cho KH, et al. Substrate spectrum extension of PenA in *Burkholderia thailandensis* with a single amino acid deletion, Glu168del. *Antimicrob Agents Chemother* 2012;56:4005–8.
31. Sha S, Zhou Y, Xin Y, Ma Y. Development of a colorimetric assay and kinetic analysis for *Mycobacterium tuberculosis*  $\alpha$ -glucose-1-phosphate thymidyltransferase. *J Biomol Screen* 2012;17:252–7.
32. Kim S, Jo S, Kim M-S, Shin DH. A study of a potent inhibitor against a GDP-6-deoxy- $\alpha$ -D-manno-heptose biosynthesis pathway as antibiotic candidates. *Microb Drug Resist* 2019; ahead of print.
33. Niyamat IB, Suhail AARS, Sandesh RJ, Habib MP. Rose Bengal sensitized niobium pentaoxide photoanode for dye sensitized solar cell application. *AIP Conference Proceedings*; 2017;1832:040022.
34. Sherman W, Day T, Jacobson MP, et al. Novel procedure for modeling ligand/receptor induced fit effects. *J Med Chem* 2006;49:534–53.
35. Jacobson MP, Pincus DL, Rapp CS, et al. A hierarchical approach to all-atom protein loop prediction. *Proteins* 2004; 55:351–67.
36. Friesner RA, Murphy RB, Repasky MP, et al. Extra precision glide: docking and scoring incorporating a model of hydrophobic enclosure for protein–ligand complexes. *J Med Chem* 2006;49:6177–96.
37. Waterhouse AM, Procter JB, Martin DMA, et al. Jalview Version 2—a multiple sequence alignment editor and analysis workbench. *Bioinformatics* 2009;25:1189–91.
38. Kim J. The use of vital dyes in corneal disease. *Curr Opin Ophthalmol* 2000;11:241–7.
39. Nakonechny F, Barel M, David A, et al. Dark antibacterial activity of Rose Bengal. *Int J Mol Sci* 2019;20:3196.
40. Ilizirov Y, Formanovsky A, Mikhura I, et al. Effect of photodynamic antibacterial chemotherapy combined with antibiotics on Gram-positive and Gram-negative bacteria. *Molecules* 2018;23:3152.
41. Schäfer M, Schmitz C, Facius R, et al. Systematic study of parameters influencing the action of Rose Bengal with visible light on bacterial cells: comparison between the biological effect and singlet-oxygen production. *Photochem Photobiol* 2000;71:514–23.
42. Nisnevitch M, Nakonechny F, Nitzan Y. Photodynamic antimicrobial chemotherapy by liposome-encapsulated water-soluble photosensitizers. *Bioorg Khim* 2010;36:396–402.
43. Nitzan Y, Nisnevitch M. Special features of Gram-positive bacterial eradication by photosensitizers. *Recent Pat Antiinfect Drug Discov* 2013;8:88–99.
44. Wu FY, Wu CW. Rose Bengal. Inhibitor of ribonucleic acid chain elongation. *Biochemistry* 1973;12:4343–8.
45. Thompson JF, Hersey P, Wachter E. Chemoablation of metastatic melanoma using intralesional Rose Bengal. *Melanoma Res* 2008;18:405–11.
46. Koevary SB. Selective toxicity of Rose Bengal to ovarian cancer cells in vitro. *Int J Physiol Pathophysiol Pharmacol* 2012; 4:99–107.
47. Fung DYC, Miller RD. Effect of dyes on bacterial growth. *Appl Environ Microbiol* 1973;25:793–9.
48. Koufen P, Zeidler U, Stark G. Photodynamic inactivation of ion channels formed by the polyene antibiotic amphotericin B in lipid membranes. *J Photochem Photobiol* 1997;38: 129–35.
49. M-Ali HA, Mohammad AS, Majed MM, et al. Modeling the effect of Rose Bengal on growth and decay patterns of *Pseudomonas aeruginosa*, *Escherichia coli* and *Staphylococcus aureus*. *IOP Conf Ser Mater Sci Eng* 2018;305:012004.
50. Nakoneczna J, Wolnikowska K, Ogonowska P, et al. Rose Bengal-mediated photoinactivation of multidrug resistant *Pseudomonas aeruginosa* is enhanced in the presence of antimicrobial peptides. *Front Microbiol* 2018;9:1949.
51. Olaitan AO, Morand S, Rolain JM. Mechanisms of polymyxin resistance: acquired and intrinsic resistance in bacteria. *Front Microbiol* 2014;5:643.
52. Norbeck DW, Rosenbrook W, Kramer JB, et al. A novel pro-drug of an impermeant inhibitor of 3-deoxy-D-manno-2-octulosonate cytidyltransferase has antibacterial activity. *J Med Chem* 1989;32:625–9.
53. Goldman RC, Capobianco JO, Doran CC, Matthyse AG. Inhibition of lipopolysaccharide synthesis in *Agrobacterium tumefaciens* and *Aeromonas salmonicida*. *J Gen Microbiol* 1992;138:1527–33.